Hindawi
International Journal of Antennas and Propagation
Volume 2019, Article ID 1687497, 9 pages
https://doi.org/10.1155/2019/1687497

Research Article

Mutual Impedance Properties in a Lossy Array Antenna

Peter L. Tokarsky

Department of Radio-Astronomical Equipment and Methods of Observation,
Institute of Radio Astronomy of the National Academy of Sciences of Ukraine, Kharkiv 61002, Ukraine

Correspondence should be addressed to Peter L. Tokarsky; p.tokarsky@rian.kharkov.ua

Received 11 August 2019; Accepted 5 October 2019; Published 11 November 2019

Academic Editor: Hervé Aubert

The impedance matrix of an arbitrary multiport array antenna with Ohmic losses was studied. It was assumed that the partial current distributions in the array, corresponding to the alternate exciting one of its terminals while the other ones are open-circuited, are known. Consideration of the power balance in the lossy array antenna has allowed ascertaining that its impedance matrix is a sum of the radiation resistance matrix and loss resistance matrix, which are in general case complex Hermitian matrices and only in some particular cases can be real. The theoretical statements obtained are confirmed by two numerical examples, where analysis of two lossy dipole arrays was performed. In the first example, the dipoles were located above the imperfect ground, which served as a source of losses, and in the second example, the same dipoles were located in free space, and the embedded parasitic element was the source of losses. The results of the analysis showed that the asymmetric placement of energy absorbers in the array antennas leads to the appearance of imaginary parts in the matrices of radiation and loss resistances, which allow one to correctly predict the behavior of the array radiation efficiency during beam scanning.

1. Introduction

The concept of mutual impedances of the circuit theory, applied to antenna problems, has been used successfully for many years to evaluate the effect of element interaction on the array antenna parameters. At first, the induced EMF method was used to calculate the mutual impedances [1–3], and then some other methods, in particular, the Poynting vector method [4–6], the variational method [7], and the integral equation method [8–10] and its modifications [11, 12]. It was generally assumed that the antennas under investigation were lossless, or the losses in them were considered very small and had no effect on the current distribution in the antennas [13, 14]. Typically, such losses were simulated by a lumped resistor connected to the antenna terminals [15], which was added to their self-impedance. In [16–20], it was shown that embedding the distributed and lumped losses into the antenna could significantly change the current distribution and, consequently, controls their parameters. In particular, in [20], using the integral equation method, it was demonstrated that by choosing the resistive loading distribution along two parallel dipoles, one can achieve a significant decrease in the mutual coupling between them.

The first attempt to study the effect of losses distributed in an array on interaction of its elements was made in [21], where it was found that loss resistances not only can be part of the self-impedance of the elements as well part of mutual impedances between them. This property of the loss resistance was confirmed by an analysis of the mutual coupling between two lossy dipoles [22], as well as by investigation of the array of vertical [23] and horizontal [24, 25] dipoles located above the imperfect ground. In recent years, in connection with the construction of new ground-based radio telescopes using large aperture arrays, as well as the reflector antennas with phased array feeds [26], explorations of the effect of losses on the different array parameters have been intensively continued [27–29]. Despite this, the mutual coupling properties in the lossy array antenna have not yet been fully studied. This article aims to partially fill this gap.

The purpose of this work is to study in detail the properties of mutual impedances between array elements with Ohmic losses and to demonstrate their use for analysis and optimal designing of the lossy array antenna. In Section 2, the basic relationships that determine the impedance matrix structure for the lossy array are derived. In Section 3, it is shown how the mutual loss resistances affect the power balance in the phased array during beam scanning, and in Section 4, two examples of numerical analysis and optimization of dipole arrays in free space and over the imperfect ground are given.

2. Theory

Consider an array antenna consisting of a set of conducting bodies located inside a bounded domain V' in free space. Assume that the medium inside V' is isotropic and linear and is characterized by the dielectric permittivity ε, magnetic permeability μ, and conductivity σ, which are scalar functions of the coordinates.

Let us suppose that the array antenna operates in the transmission mode and is fed by the harmonic oscillators (with the time dependence $e^{j\omega t}$) by means of N regular TEM-transmission lines. We will take the reference planes in these lines as N array ports. Since the currents and voltages can be uniquely determined at these ports, the terminal equation of the array antenna can be written in the form

$$\mathbf{v} = \mathbf{Z}\mathbf{i}, \tag{1}$$

where $\mathbf{i}$ and $\mathbf{v}$ are the vectors of complex amplitudes of the currents and voltages at the array ports and $\mathbf{Z}$ is an array antenna impedance matrix.

Assume also that we know the N partial current distributions $\vec{J}_n(\vec{R'})$ fields $\vec{E}_n(\vec{R})$ and $\vec{H}_n(\vec{R})$ radiated by them, which are found as results of solving N electromagnetic boundary-value problems, when all array ports are excited one after another by current i_n $(n = 1, \dots, N)$, while the other ports are open-circuited ($i_m = 0$, $m = 1, \dots, N$, $m \neq n$), where $\vec{R'}$ and $\vec{R}$ are position vectors of a source point and observation point, respectively. Note that these currents should be determined by taking into account the environment of the array, which plays an essential role in the radiation process, and to which belong parasitic elements, ground, screens, a dielectric substrate, and so on.

The domain V'_n of function $\vec{J}_n(\vec{R'})$ coupled with the nth array port, in fact, is an nth embedded element in the array with all other elements open circuited.

The current $\vec{J}_n(\vec{R'})$ can be presented as follows:

$$\vec{J}_n\left(\vec{R'}\right) = i_n \frac{1}{S_n} \vec{\upsilon}_n\left(\vec{R'}\right), \quad \vec{R'} \in V'_n, \tag{2}$$

where $\vec{\upsilon}_n(\vec{R'})$ is the dimensionless vector function characterizing the distribution of the electric current in the domain V'_n, S_n is the cross section of the current at the nth terminal, and $V'_1 \cup V'_2 \cup \cdots \cup V'_N = V'$ is the domain occupied by all embedded elements.

When all array ports are excited simultaneously, the total current density $\vec{J}(\vec{R'})$ in the domain V' and the total fields $\vec{E}(\vec{R})$ and $\vec{H}(\vec{R})$ they produced are defined as the sum:

$$\vec{J}\left(\vec{R'}\right) = \sum_{n=1}^{N} \vec{J}_n\left(\vec{R'}\right), \tag{3}$$

$$\begin{aligned} \vec{E}(\vec{R}) &= \sum_{n=1}^{N} \vec{E}_n(\vec{R}), \\ \vec{H}(\vec{R}) &= \sum_{n=1}^{N} \vec{H}_n(\vec{R}). \end{aligned} \tag{4}$$

Grounding on these assumptions, let us determine the impedance at the array antenna ports using the Poynting theorem. To do this, we surround the entire array with a spherical surface S_{ext} located in the far zone and consider the region V bounded from the outside by surface S_{ext}, and from the inside with surface S_{int}, which is formed by the reference planes S'_n in the transmission lines selected as the array ports ($S_{\text{int}} = S'_1 \cup S'_2 \cup \cdots \cup S'_N$).

External sources of currents and fields are absent in V, so the power balance equation here has the form

$$\frac{1}{2}\int_{V'} \frac{\vec{J} \cdot \vec{J}^*}{\sigma} dV' + \frac{1}{2}\int_{S_{\text{ext}}} \left[\vec{E} \times \vec{H}^*\right] \cdot \hat{s}\, dS + \frac{1}{2}\int_{S_{\text{int}}} \left[\vec{E} \times \vec{H}^*\right] \cdot \hat{s} dS + \frac{j\omega}{2}\int_{V} \left(\mu \vec{H} \cdot \vec{H}^* - \varepsilon \vec{E} \cdot \vec{E}^*\right) dV = 0, \tag{5}$$

where $\hat{s}$ is the outward-directed unit normal to surface $S = S_{\text{ext}} \cup S_{\text{int}}$ and "$*$" denotes complex conjugation.

The first term in (5) determines the lost power P_{l}, scattered in volume V' in the form of heat. Using relations (1)–(3), we express this power through the currents at the array ports:

$$P_{\text{l}} = \frac{1}{2}\int_{V'} \frac{\vec{J}^*\left(\vec{R'}\right) \cdot \vec{J}\left(\vec{R'}\right)}{\sigma\left(\vec{R'}\right)} dV' = \frac{1}{2} \mathbf{i}_{\text{t}}^* \mathbf{Z}_{\text{l}} \mathbf{i}, \tag{6}$$

where the subscript t denotes transposition and $\mathbf{Z}_{\text{l}}$ is a loss resistance matrix of the array antenna, in which elements are determined as

$$Z_{\text{l}mn} = \int_{V'} \frac{\vec{\upsilon}^*_m\left(\vec{R'}\right) \cdot \vec{\upsilon}_n\left(\vec{R'}\right)}{S_m S_n \sigma\left(\vec{R'}\right)} dV'. \tag{7}$$

From (6) and (7), $\mathbf{Z}_{\text{l}}$ is a Hermitian non-negative definite matrix. Its diagonal elements $Z_{\text{l}nn}$ are real non-negative numbers equal to the powers of the thermal losses of the array when its ports are alternately excited by the unit current that allows to call them as self-loss resistances. Each off-diagonal element $Z_{\text{l}mn}$ is a mutual loss resistance being a measure of nonorthogonality of the two vector functions $\vec{J}_m(\vec{R'})$ and $\vec{J}_n(\vec{R'})$ with respect to their weighted inner product (7).

The second term in (5) determines the power P_r radiated by the array antenna that can be represented as

$$P_r = \frac{1}{2}\int_{S_{ext}}\left[\overrightarrow{\mathbf{E}} \times \overrightarrow{\mathbf{H}^*}\right]\cdot \hat{R}dS = \frac{1}{2}\,\mathbf{i}_t^*\mathbf{Z}_r\mathbf{i}, \tag{8}$$

where $\mathbf{Z}_r$ is a radiation resistance matrix, $\overrightarrow{\mathbf{E}}$ and $\overrightarrow{\mathbf{H}}$ are the far-field vectors related as $Z_0\overrightarrow{\mathbf{H}} = [\widehat{\mathbf{R}} \times \overrightarrow{\mathbf{E}}]$, and Z_0 is the intrinsic free space impedance.

Matrix $\mathbf{Z}_r$ can be determined if we substitute (4) in (8) and take into account that the embedded element patterns can be represented [30].

$$\overrightarrow{E_n}(R,\theta,\varphi) = ji_n\frac{l_{en}Z_0}{2\lambda}\frac{e^{-jkR}}{R}\overrightarrow{F_n}(\theta,\varphi), \tag{9}$$

where l_{en} is the effective length, λ is the wavelength, (R,θ,φ) are the observation point coordinates, and $\overrightarrow{F_n}(\theta,\varphi)$ is the embedded element normalized pattern, given by [31]:

$$\overrightarrow{F_n}(\theta,\varphi) = \frac{1}{l_{en}S_{in}}\int_{V'}\left[\widehat{\mathbf{R}}\times\left[\widehat{\mathbf{R}}\times\overrightarrow{v}_n\left(\overrightarrow{R'}\right)\right]\right]e^{jk\widehat{R}\cdot\left(\overrightarrow{R'}\right)}dV'. \tag{10}$$

$\widehat{\mathbf{R}}$ is the unit vector in (θ,φ) direction.

As a result, we find the radiation resistance matrix elements:

$$Z_{rmn} = \frac{Z_0}{4}\frac{l_{em}l_{en}}{\lambda^2}\int_0^{2\pi}\int_0^{\pi}\overrightarrow{F}^*_m(\theta,\varphi)\overrightarrow{F_n}(\theta,\varphi)\sin\theta\, d\theta\, d\varphi. \tag{11}$$

Before, the same equation was derived in [4] to determine the mutual resistance between two arbitrary lossless antennas.

Comparing (11) and (7), it can easily be seen that $\mathbf{Z}_r$, as well as $\mathbf{Z}_l$, is the Hermitian matrix, which is positive-definite since $P_r > 0$ for any radiating systems. Its diagonal elements Z_{rnn} are real positive numbers, which are the self-radiation resistances of the array antenna, and the off-diagonal elements Z_{rnm} are mutual radiation resistances and determine the measure of the nonorthogonality of the embedded element normalized patterns $\overrightarrow{F_m}(\theta,\varphi)$ and $\overrightarrow{F_n}(\theta,\varphi)$.

The third term in (5), taken with the opposite sign, describes the power P_s entering the array antenna from external sources through the ports. It can also be represented by the sum:

$$P_s = -\frac{1}{2}\sum_{n=1}^{N}\int_{S_n}\left[\overrightarrow{E}\times\overrightarrow{\mathbf{H}^*}\right]\hat{s}dS = \frac{1}{2}\sum_{n=1}^{N}V_nI_n^* = \frac{1}{2}\mathbf{i}_t^*\mathbf{Z}\mathbf{i}, \tag{12}$$

where $\mathbf{Z}$ is the array antenna impedance matrix (1).

The fourth term describes the reactive power P_Q produced by the array in domain V. Taking (3) and (4) into account, this power can be represented as the sum:

$$P_Q = \frac{j\omega}{2}\sum_{m=1}^{N}\sum_{n=1}^{N}\int_V\left(\mu\overrightarrow{H_n}\cdot\overrightarrow{H}^*_m - \varepsilon\overrightarrow{E_n}\cdot\overrightarrow{E}^*_m\right)dV = j\frac{1}{2}\mathbf{i}_t^*\mathbf{X}_Q\mathbf{i}, \tag{13}$$

where $\mathbf{X}_Q$ is an array antenna reactance matrix [4, 5].

Now, substituting (6), (8), (12), and (13) in (5) and assuming $\mathbf{i} \neq 0$, we can derive the following equation:

$$P_l + P_r + jP_Q = P_s, \tag{14}$$

which can be divided into two equations

$$P_l + P_r = \mathrm{Re}(P_s) = P_{in}, \tag{15}$$

$$P_Q = \mathrm{Im}(P_s), \tag{16}$$

where P_{in} is the array antenna input power.

From (14) follows the equation

$$\mathbf{Z}_l + \mathbf{Z}_r + j\mathbf{X}_Q = \mathbf{Z}, \tag{17}$$

and from (15) and (16), the following equations are obtained:

$$\begin{aligned}\mathbf{R} &= \mathrm{Re}(\mathbf{Z}) = \mathbf{Z}_l + \mathbf{Z}_r,\\ \mathbf{X} &= \mathrm{Im}(\mathbf{Z}) = \mathbf{X}_Q.\end{aligned} \tag{18}$$

Since the matrices $\mathbf{Z}_r$ and $\mathbf{Z}_l$ are Hermitian, each of them can be divided into a symmetric real part and an antisymmetric imaginary part, namely,

$$\begin{aligned}\mathbf{Z}_r &= \mathbf{R}_r + j\mathbf{R}''_r,\\ \mathbf{Z}_l &= \mathbf{R}_l + j\mathbf{R}''_l.\end{aligned} \tag{19}$$

Using the reciprocity principle, it is not difficult to prove that

$$\mathrm{Im}(\mathbf{Z}_r + \mathbf{Z}_l) = \mathbf{R}''_r + \mathbf{R}''_l = 0, \tag{20}$$

and $\mathbf{X}_Q$ is a real symmetric matrix.

From (20),

$$\mathbf{R}''_r = -\mathbf{R}''_l = \mathbf{R}'', \tag{21}$$

that allows us to write (19) as

$$\begin{aligned}\mathbf{Z}_r &= \mathbf{R}_r + j\mathbf{R}'',\\ \mathbf{Z}_l &= \mathbf{R}_l - j\mathbf{R}''.\end{aligned} \tag{22}$$

3. Discussion

Let us consider what influence the self and mutual losses resistances exert on a power balance in a lossy array antenna with phase steering on the example of a uniformly spaced N-element linear array. The Joule losses on it can be due to the finite conductivity of the material, the presence of embedded resistors, or the presence of closely located absorbing bodies or surfaces (array construction, aircraft body, passive scatterers, imperfect ground, etc.). We suppose that its matrices are known from the boundary problem solution, taking into account the loss distribution. In addition, the array ports are excited by currents $\mathbf{i}$ of the uniform amplitude i_0 with a progressive phase shift Δ, i.e., $i_n = i_0 e^{jn\Delta}$. Then, the input power is

$$P_{\text{in}} = \frac{i_0^2}{2}\sum_{n=1}^{N} R_{nn} + i_0^2 \sum_{m=2}^{N}\sum_{n=1}^{m-1} R_{mn}\cos(m-n)\Delta = P_{\text{in}}^0 + P_{\text{in}}', \tag{23}$$

and the radiated P_{r} and lost P_{l} powers are

$$P_{\text{r(l)}} = \frac{i_0^2}{2}\sum_{n=1}^{N} R_{\text{r(l)}nn} + i_0^2 \sum_{m=2}^{N}\sum_{n=1}^{m-1} R_{\text{r(l)}mn}\cos(m-n)\Delta$$
$$\pm\, i_0^2 \sum_{m=2}^{N}\sum_{n=1}^{m-1} R_{mn}''\sin(m-n)\Delta = P_{\text{r(l)}}^0 + P_{\text{r(l)}}' \pm P'', \tag{24}$$

where the "plus" sign before P'' pertains to the radiation power and the "minus" sign to the loss power. From (24), both powers P_{r} and P_{l} consist of three terms. The first of these, P^0 is determined only by the self-resistances $R_{\text{r(l)}nn}$ and does not depend on Δ. The second P' and the third P'', being terms in (24), are determined by the real and imaginary parts of mutual resistances $Z_{\text{r(l)}mn}$ and are the even and the odd functions of Δ, respectively. When P'' is changed, the input power P_{in} remains unchanged and is redistributed between the radiation power P_{r} and the loss power P_{l}, herewith when one of them increases by P'', the other decreases by the same amount. This effect occurs in all multiport radiating systems with nonuniform loss distribution.

4. Numerical Examples

4.1. Dipole Array over Lossy Half-Space. Consider an array of two closely spaced identical symmetrical dipoles located in the immediate vicinity of the surface of a plane imperfect ground with parameters $\varepsilon_{\text{r}} = 13$ and $\sigma = 0.005$ S/m (average ground). The $\lambda/2$-long dipoles are made of a thin, perfectly conducting wire with a diameter of 0.001λ and are oriented along the Y-axis of the Cartesian coordinates. Consider the two variants for arranging the dipoles above the ground, one-level array (Figure 1(a)) and two-level array (Figure 1(b)). In both arrays, dipole 1 is located at the height $h = \lambda/4$, and the distance between the dipoles is $d = \lambda/8$. The first array is named usually as a broadside array (BSA) and the second one as an end-fire array (EFA).

Matrices $\mathbf{Z}$, $\mathbf{Z}_{\text{r}}$, and $\mathbf{Z}_{\text{l}}$ for both arrays were determined with the full-wave simulation NEC-2 software [32], based on the moment method [33]. All calculations were performed at 50 MHz; each dipole was divided into 46 segments. A detailed technique of computing the impedance matrices of lossy wire arrays is given in [34] and was successfully used in [35, 36]. The matrices found are as follows:

(i) For the BSA (Figure 1(a)),

$$\mathbf{Z} = \begin{pmatrix} 95.719 + \text{j}59.173 & 86.911 + \text{j}6.761 \\ 86.911 + \text{j}6.761 & 95.719 + \text{j}59.173 \end{pmatrix}, \tag{25}$$

$$\mathbf{Z}_{\text{r}} = \begin{pmatrix} 69.210 & 63.506 \\ 63.506 & 69.210 \end{pmatrix}, \tag{26}$$

$$\mathbf{Z}_{\text{l}} = \begin{pmatrix} 26.509 & 23.405 \\ 23.405 & 26.509 \end{pmatrix}. \tag{27}$$

(ii) For the EFA (Figure 1(b)),

$$\mathbf{Z} = \begin{pmatrix} 96.051 + \text{j}61.135 & 71.639 + \text{j}14.84 \\ 71.639 + \text{j}14.84 & 68.273 + \text{j}60.752 \end{pmatrix}, \tag{28}$$

$$\mathbf{Z}_{\text{r}} = \begin{pmatrix} 68.07 & 44.995 - \text{j}11.594 \\ 44.995 + \text{j}11.594 & 32.137 \end{pmatrix}, \tag{29}$$

$$\mathbf{Z}_{\text{l}} = \begin{pmatrix} 27.981 & 26.644 + \text{j}11.594 \\ 26.644 - \text{j}11.594 & 36.136 \end{pmatrix}. \tag{30}$$

Matrices $\mathbf{Z}_{\text{r}}$ and $\mathbf{Z}_{\text{l}}$ of the BSA are real and symmetric concerning the main and secondary diagonals since the array is symmetric concerning the coordinate plane $X = 0$. The EFA dipoles are located at different distances from the ground surface, which affect their parameters in different ways, so the self-resistances of the dipoles are not the same, and the mutual radiation and loss resistances have the imaginary parts of $\pm R''$. Substituting (25)–(30) into (23) and (24), we find dependencies of the powers P_{in}, P_{r}, and P_{l} on Δ and represent them in a normalized form.

(i) For the BSA,

$$\begin{aligned} \widetilde{P}_{\text{in}}(\Delta) &= 1 + 0.908\cos\Delta, \\ \widetilde{P}_{\text{r}}(\Delta) &= 0.723 + 0.663\cos\Delta, \\ \widetilde{P}_{\text{l}}(\Delta) &= 0.277 + 0.245\cos\Delta. \end{aligned} \tag{31}$$

(ii) For the EFA,

$$\widetilde{P}_{\text{in}}(\Delta) = 1 + 0.872\cos\Delta, \tag{32}$$

$$\widetilde{P}_{\text{r}}(\Delta) = 0.610 + 0.548\cos\Delta + 0.141\sin\Delta, \tag{33}$$

$$\widetilde{P}_{\text{l}}(\Delta) = 0.390 + 0.324\cos\Delta - 0.141\sin\Delta, \tag{34}$$

where $\widetilde{P} = P/P_0$ and $P_0 = (R_{11} + R_{22})i_0^2/2$.

Figure 2 shows the radiation efficiency.

$$\eta_{\text{r}} = \frac{\mathbf{i}_{\text{t}}^*\mathbf{Z}_{\text{r}}\mathbf{i}}{\mathbf{i}_{\text{t}}^*\mathbf{R}\mathbf{i}} = \frac{\widetilde{P}_{\text{r}}(\Delta)}{\widetilde{P}_{\text{in}}(\Delta)}, \tag{35}$$

for each of the arrays as functions of Δ, as well as the single dipole efficiency ($=0.723$). The BSA efficiency has a

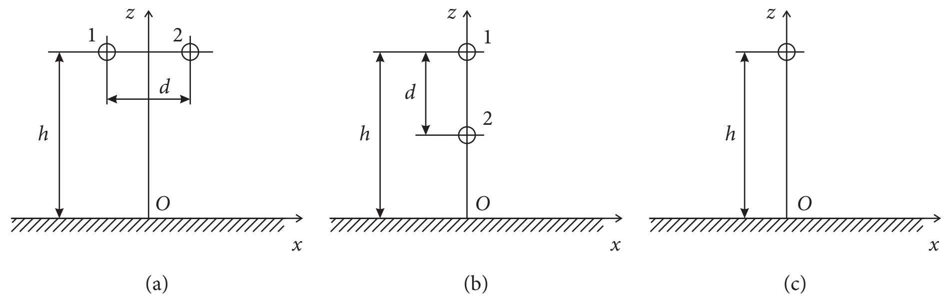

Figure 1: Dipole array structure: (a) one-level array (BSA); (b) two-level array (EFA); (c) single dipole.

maximum of 0.727 when the dipoles are excited in-phase. It is practically constant in the range of 200°, differing little from the single dipole efficiency, and only near to ±180°, it decreases to 0.648, i.e., by 0.5 dB. The EFA radiation efficiency, on the contrary, strongly depends on Δ, varying from 0.256 at −156° to 0.848 at 144°, which is more than 5 dB.

The found boundaries of the change in the efficiency of both arrays are valid only for the uniform amplitude excitation of dipoles. Using the methods for solving the eigenvalue problems [37], we found the extreme values of the radiation efficiency (33) for both arrays. For the BSA, they turned out to be the same as in Figure 2. A similar result of radiation efficiency optimization was obtained in [14] for BSA of printed dipoles.

In contrast, the total range of variation in the EFA efficiency was much wider than shown in Figure 2. Its extreme values are $\eta_r^{\max} = 0.8803$ and $\eta_r^{\min} = 0.0228$. The last value attracts special attention since it indicates that the power supplied into the array antenna from external sources practically does not radiate into free space and almost entirely (97.72%) penetrates into the ground. Thus, the air-ground interface is practically transparent for the field of this array.

The currents at the EFA ports providing extreme efficiency values are the eigenvectors of the pencil of Hermitian forms (33). We had computed these currents using the MathCad and present them in the normalized form:

$$\mathbf{i}^{\max} = \begin{pmatrix} 1 \\ 0.7677\angle 147,3^\circ \end{pmatrix},$$
$$\mathbf{i}^{\min} = \begin{pmatrix} 0.6813\angle 165.1^\circ \\ 1 \end{pmatrix}. \tag{36}$$

Figure 3 shows the EFA gain patterns in the E and H planes, calculated using NEC-2 software. Here, the two upper curves refer to the EFA with the maximum radiation efficiency and the two lower curves to the EFA with the minimum radiation efficiency. The difference between the gains in the zenith direction is close to 14 dB.

The extremely low EFA gain with minimal efficiency once again confirms that the radiated power near completely goes into the bottom half-space. This array antenna property perhaps could be useful when creating the GPR.

4.2. Dipole Array with Lossy Parasitic Element. Analyzing the results of the previous numerical example, one may suspect

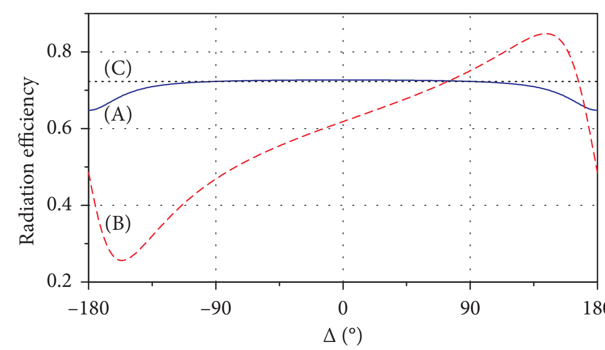

Figure 2: Efficiency vs. phase Δ for both arrays: (A) BSA, (B) EFA, and (C) for a single dipole.

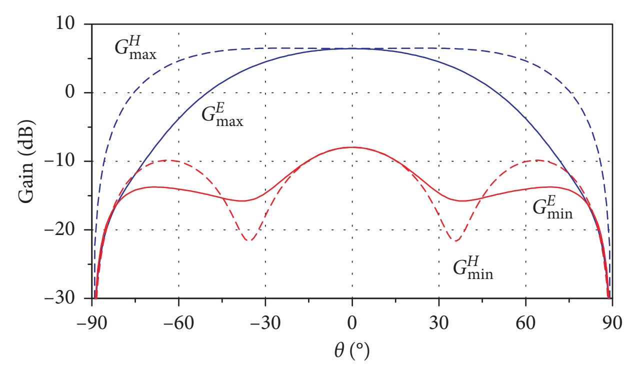

Figure 3: Gain patterns of the EFA with maximum and minimum radiation efficiencies.

that appreciable values of the imaginary components in the mutual radiation (and loss) resistances between the array elements, which significantly affect the radiation efficiency, can arise only when nearby there is some very large absorber alike the lossy half-space. To dispel such suspicions, consider an example of a simple array antenna with a small absorber that allows making analytical evaluations.

Consider the same two dipole arrays as in the previous example (Figures 1(a) and 1(b)); however, we will remove the imperfect ground from consideration and add the third dipole instead it, identical to dipoles 1 and 2, that is loaded with impedance Z_L (Figures 4(a) and 4(b)). Thus, each of the newly created arrays consists of two driven dipoles 1 and 2 located near a parasitic dipole, which also participates in the process of electromagnetic wave radiation. For brevity, we will call the dipole array shown in Figure 4(a) horizontal (H-

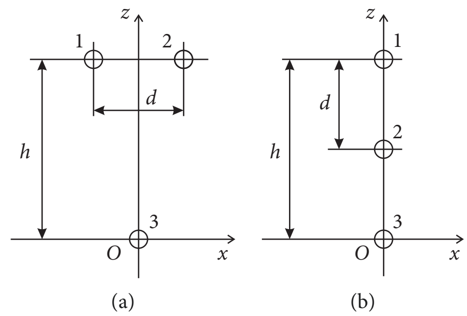

Figure 4: Dipole arrays in free space: (a) H-array; (b) V-array.

array) and in Figure 4(b) vertical (V-array). As before, we will assume that all dipoles are perfectly conducting and losses are concentrated only in the load Z_L ($\mathrm{Re}\, Z_L > 0$).

These array antennas are simple enough to derive analytical expressions for calculating their impedance matrices and loss resistance matrices. For this purpose, we consider some array consisting of two excited dipoles and a third passive one, in which the terminal currents and voltages satisfy the following Carter equations:

$$\begin{aligned} v_1 &= \widehat{Z}_{11} i_1 + \widehat{Z}_{12} i_2 + \widehat{Z}_{13} i_3, \\ v_2 &= \widehat{Z}_{21} i_1 + \widehat{Z}_{22} i_2 + \widehat{Z}_{23} i_3, \\ v_3 &= \widehat{Z}_{31} i_1 + \widehat{Z}_{32} i_2 + \widehat{Z}_{33} i_3, \end{aligned} \quad (37)$$

where $\widehat{Z}_{mn}$ are the self and mutual impedances between the dipoles (m, $n = 1, 2, 3$).

Given that $v_3 = -Z_L i_3$, we express the current i_3 through the currents i_1 and i_2

$$i_3 = \alpha i_1 + \beta i_2, \quad (38)$$

where

$$\begin{aligned} \alpha &= -\frac{\widehat{Z}_{31}}{\widehat{Z}_{33} + Z_L}, \\ \beta &= -\frac{\widehat{Z}_{32}}{\widehat{Z}_{33} + Z_L}, \end{aligned} \quad (39)$$

and exclude the variables v_3, i_3 from the equation (37); as a result, it is transformed to the following form:

$$\begin{aligned} v_1 &= Z_{11} i_1 + Z_{12} i_2, \\ v_2 &= Z_{21} i_1 + Z_{22} i_2, \end{aligned} \quad (40)$$

where Z_{mn} are the desired impedances of a two-element array with the embedded parasitic element:

$$\begin{aligned} Z_{11} &= \widehat{Z}_{11} + \widehat{Z}_{13}\alpha, \\ Z_{12} &= \widehat{Z}_{12} + \widehat{Z}_{13}\beta, \\ Z_{21} &= \widehat{Z}_{21} + \widehat{Z}_{23}\alpha, \\ Z_{22} &= \widehat{Z}_{22} + \widehat{Z}_{23}\beta. \end{aligned} \quad (41)$$

Now, we find the lost power P_l in the array antenna absorbed by the load Z_L:

$$\begin{aligned} P_l &= \frac{1}{2}|i_3|^2 R_L = \frac{1}{2}\left(\alpha^* i_1^* + \beta^* i_2^*\right)\left(\alpha i_1 + \beta i_2\right) R_L = \\ &= \frac{1}{2}\left(\alpha^* \alpha i_1^* i_1 + \beta^* \alpha i_2^* i_1 + \alpha^* \beta i_1^* i_2 + \beta^* \beta i_2^* i_2\right) R_L. \end{aligned} \quad (42)$$

The right side of equation (42) is a Hermitian form (6), in which coefficients are the mutual loss resistances of the array antenna:

$$\begin{aligned} Z_{l11} &= |\alpha|^2 R_L, \\ Z_{l12} &= \alpha^* \beta R_L, \\ Z_{l21} &= \beta^* \alpha R_L, \\ Z_{l22} &= |\beta|^2 R_L. \end{aligned} \quad (43)$$

To apply equations (41) and (43) to determine the matrices $\mathbf{Z}$ and $\mathbf{Z}_l$ of the H- and V-array, we need their impedance matrices $\widehat{\mathbf{Z}}$ (37). As in the previous example, we calculated them using the full-wave simulation NEC-2 software. Their elements found are as follows:

(i) For the H-array (Figure 4(a)),

$$\begin{aligned} \widehat{Z}_{11} &= \widehat{Z}_{22} = 81.268 + j44.175, \\ \widehat{Z}_{33} &= 79.065 + j47.759, \\ \widehat{Z}_{21} &= 71.104 - j7.539, \\ \widehat{Z}_{31} &= \widehat{Z}_{32} = 38.251 - j40.480. \end{aligned} \quad (44)$$

(ii) For the V-array (Figure 1(b)),

$$\begin{aligned} \widehat{Z}_{11} &= \widehat{Z}_{33} = 81.045 + j43.982, \\ \widehat{Z}_{22} &= 83.276 + j40.574, \\ \widehat{Z}_{21} &= \widehat{Z}_{32} = 71.236 - j9.650, \\ \widehat{Z}_{31} &= 42.188 - j41.008. \end{aligned} \quad (45)$$

The remaining elements of $\widehat{\mathbf{Z}}$ matrices are determined using the property of their symmetry.

Now, substituting (44) and (45) into (41) and (43), we find the matrices $\mathbf{Z}$ and $\mathbf{Z}_l$:

(i) For the H-array (Figure 4(a)),

$$\mathbf{Z} = \begin{pmatrix} 82.379 + j63.759 & 72.214 + j12.045 \\ 72.214 + j12.045 & 82.379 + j63.759 \end{pmatrix}, \tag{46}$$

$$\mathbf{Z}_{\mathrm{r}} = \begin{pmatrix} 72.571 & 62.406 \\ 62.406 & 72.571 \end{pmatrix}, \tag{47}$$

$$\mathbf{Z}_{\mathrm{l}} = \begin{pmatrix} 9.808 & 9.808 \\ 9.808 & 9.808 \end{pmatrix}. \tag{48}$$

(ii) For the V-array (Figure 4(b)),

$$\mathbf{Z} = \begin{pmatrix} 80.440 + j65.329 & 55.136 + j10.884 \\ 55.136 + j10.884 & 52.544 + j49.056 \end{pmatrix}, \tag{49}$$

$$\mathbf{Z}_{\mathrm{r}} = \begin{pmatrix} 69.762 & 44.645 - j7.755 \\ 44.645 + j7.755 & 36.603 \end{pmatrix}, \tag{50}$$

$$\mathbf{Z}_{\mathrm{l}} = \begin{pmatrix} 10.678 & 10.491 + j7.755 \\ 10.491 - j7.755 & 15.941 \end{pmatrix}. \tag{51}$$

Let us collate the calculated matrices $\mathbf{Z}_{\mathrm{r}}$ and $\mathbf{Z}_{\mathrm{l}}$ with their counterparts from the previous example. Comparing the $\mathbf{Z}_{\mathrm{r}}$ matrices, (47) with (26), as well as (50) with (29), it is easy to see that each pair of matrices has not only the same structure but also has elements of similar magnitude, the difference between which does not exceed 2–4 Ohms. A similar comparison of the loss resistance matrices $\mathbf{Z}_{\mathrm{l}}$, (48) with (27) and (51) with (30), shows that they also have the same structure, but they noticeably differ in magnitude, the elements of these matrices for array antennas in free space are about 2-3 times less than for arrays above the imperfect ground. Such a difference does not seem very large if we take into account the dissimilarity in the absorbing abilities of the lossy half-space and the single lumped resistor.

The resulting matrices $\mathbf{Z}$, $\mathbf{Z}_{\mathrm{r}}$, and $\mathbf{Z}_{\mathrm{l}}$ (46)–(51) make it possible to calculate all power characteristics of the array antennas under consideration as in the previous example. Here are just a few of them. Figure 5 shows the dependences of the radiation efficiency of the uniform amplitude arrays on the phase shift Δ between their terminal currents.

Comparing Figure 5 with Figure 2, it is easy to see that the behaviors of the H-array efficiency and the BSA efficiency are directly opposite. The H-array excited in-phase has a minimum efficiency of 0.8731, while the in-phase excited BSA has maximum efficiency. With an increase in the phase shift, the H-array efficiency increases, reaching 1 at $\Delta = \pm 180^\circ$, and the BSA radiation efficiency decreases, reaching a minimum at $\Delta = \pm 180^\circ$. The noted difference in the behavior of the efficiency of these arrays is easily explained by the fact that the H-array losses are concentrated at one point, and the BSA losses are distributed in an infinitely large volume. The radiation fields of the antiphase excited dipoles 1 and 2 of the H-array ($i_1 = -i_2$, $|\Delta| = 180^\circ$) induce in the dipole 3 the equal currents with opposite directions, which are reciprocally compensated and do not produce power losses in Z_{L}, so the array antenna efficiency is 1. When Δ different from 180°, a current appears in dipole 3, the amplitude of which increases with decreasing Δ and reaches a maximum at $\Delta = 0$, creating the maximum power loss in the load and thereby causing the minimum efficiency of the H-array. Variations in BSA efficiency with a change in Δ have another nature; they are associated with the redistribution of the array radiation power between space and ground waves [38, 39]. The ground wave is absorbed more strongly by the imperfect ground than the space wave. With an increase of Δ, the part of the radiated power carried by the ground wave increases, reaching a maximum at $\Delta = \pm 180^\circ$, which minimizes the BSA radiation efficiency.

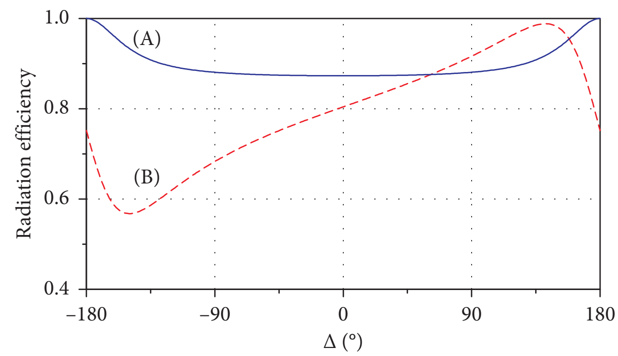

Figure 5: Dependences of the radiation efficiency from phase Δ for both arrays: (A) H-array; (B) V-array.

Now, we compare the behaviors of the radiation efficiencies of the V-array and EFA when Δ changes. Looking at Figures 2 and 5, where these dependencies are given, it becomes obvious that the curves (B) on them are almost identical in shape, but the curve for the V-array is shifted up about 0.2 in reference to the curve for the EFA. The efficiency values at the minimum and maximum points of the curve (B) in Figure 5 are 0.5678 and 0.9884, respectively, and their positions are $\Delta_{\min} = -150^\circ$ and $\Delta_{\max} = 142^\circ$, accurate to a few degrees; they coincide with the positions of the extrema of the compared curve (B) in Figure 2.

The reasons for the appearance of the curve extrema in the specified positions on the graph are easy to explain from a physical point of view. Figure 6 shows two gain patterns $G_E^{\max}$ and $G_E^{\min}$ in the E-plane of the V-array, calculated using the NEC-2 software. The amplitudes of the excitation currents of the array ports are identical, and their phases correspond to the radiation efficiency extrema in Figure 5.

The $G_E^{\max}$ pattern is oriented so that its main beam is directed along the Z-axis, and its minimum is directed towards the parasitic element, as a result of which a very small current is induced in it, which leads to negligible losses in the load Z_{L} and to the maximum array radiation efficiency. In contrast, the main beam of the $G_E^{\min}$ pattern is directed towards the parasitic element, where intense currents are induced, causing the maximum power loss in the load, which causes the minimum array radiation efficiency. Note that the extreme values of this array radiation efficiency obtained in the process of full-wave modeling coincide with the extrema

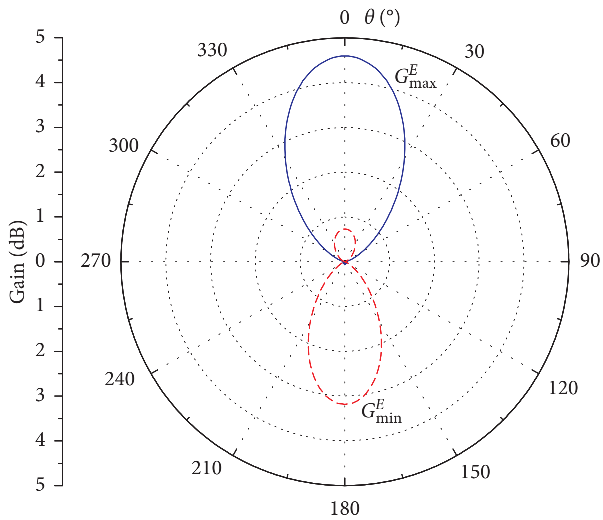

Figure 6: Gain patterns of the V-array with maximum and minimum radiation efficiencies.

of the curve (B), which was calculated using the self and mutual radiation resistances (50). The imaginary parts of the mutual radiation resistances made a significant contribution to the formation of the dependence of the radiation efficiencies on Δ in Figure 5 as well as in Figure 2; without them, the calculation results would be incorrect.

The absolute extrema values of the V-array radiation efficiencies found from solving the eigenvalue problem are $\eta_r^{\max} = 1$ and $\eta_r^{\min} = 0.4215$, which are implemented with the following currents:

$$\mathbf{i}^{\max} = \begin{pmatrix} 1 \\ 0.8184\angle 143.5^\circ \end{pmatrix},$$
$$\mathbf{i}^{\min} = \begin{pmatrix} 0.6349\angle 160.1^\circ \\ 1 \end{pmatrix}. \quad (52)$$

Note that the efficiency of this array antenna, in contrast to the EFA, can reach 100%; however, it is not possible to get such a deep minimum as in the EFA, which, however, is not surprising, comparing the absorption capacity of the lumped load and imperfect ground.

5. Conclusions

The analysis of the power balance in the lossy array antenna made it possible to study the properties of mutual impedances between its terminals. It is shown that the mutual impedance real part in the general case is the sum of complex mutual radiation resistance and complex mutual loss resistance. The imaginary parts of these resistances are equal in magnitude and opposite in sign. They allow to estimate the redistribution of the array input power between the radiation power and the lost power when the phase of the currents at the array terminals change, but they are in no way related to the reactive power of the array antenna. The results of the numerical analysis of two dipole arrays over imperfect ground and in free space have convincingly proved that it is the presence of imaginary components in the mutual radiation and loss resistances that allow to correctly evaluate the behavior of their radiation efficiency at beam scanning.

Data Availability

The data used to support the findings of this study are available from the corresponding author upon request.

Conflicts of Interest

The author declares that he has no conflicts of interest.

References

[1] A. A. Pistolkors, "The radiation resistance of beam antennas," *Proceedings of the IRE*, vol. 17, no. 3, pp. 562–579, 1929.

[2] R. Bechmann, "On the calculation of radiation resistance of antennas and antenna combinations," *Proceedings. IRE*, vol. 19, no. 8, pp. 1471–1480, 1931.

[3] P. S. Carter, "Circuit relations in radiating systems and applications to antenna problems," *Proceedings of the IRE*, vol. 20, no. 6, pp. 1004–1041, 1932.

[4] O. G. Vendik, "Determination of a mutual impedance between antennas using known far-field radiation patterns," *Radiotekhnika*, vol. 17, no. 10, pp. 11–20, 1962, in Russian.

[5] O. G. Vendik and D. S. Kozlov, "A novel method for the mutual coupling calculation between antenna array radiators: analysis of the radiation pattern of a single radiator in the antenna array," *IEEE Antennas and Propagation Magazine*, vol. 57, no. 6, pp. 16–21, 2015.

[6] W. Wasylkiwskyj and W. K. Kahn, "Theory of mutual coupling among minimum-scattering antennas," *IEEE Transactions on Antennas and Propagation*, vol. 18, no. 2, pp. 204–216, 1970.

[7] J. V. Surutka, "Self and mutual impedances of two parallel staggered dipoles by variational method," *Radio and Electronic Engineer*, vol. 41, no. 6, pp. 257–264, 1971.

[8] H. C. Pocklington, "Electrical oscillations in wires," *Proceedings of the Cambridge Philosophical Society*, vol. 9, pp. 324–333, 1897.

[9] E. Hallén, "Theoretical investigations into the transmitting and receiving antennae," *Nova Acta Regiae Societatis Scientiarum Upsaliensis, Ser. 4*, Almqvist & Wiksell, vol. 11, no. 4, pp. 1–44, Stockholm, Sweden, 1938.

[10] K. Mei, "On the integral equations of thin wire antennas," *IEEE Transactions on Antennas and Propagation*, vol. 13, no. 3, pp. 374–378, 1965.

[11] R. W. P. King, B. B. Mack, and S. S. Sandler, *Array of Cylindrical Dipoles*, Cambridge University Press, New York, NY, USA, 1968.

[12] J. L. Pages, "Moment method evaluation of mutual impedance between dipoles," *Journal Electrical and Electronics Engineering, Australia*, vol. 1, no. 1, pp. 69-70, 1981.

[13] E. Newman and P. Tulyathan, "Analysis of microstrip antennas using moment methods," *IEEE Transactions on Antennas and Propagation*, vol. 29, no. 1, pp. 47–53, 1981.

[14] D. Pozar, "Considerations for millimeter wave printed antennas," *IEEE Transactions on Antennas and Propagation*, vol. 31, no. 5, pp. 740–747, 1983.

[15] G. Delisle, M. Pelletier, and J. Cummins, "Signal-to-noise ratios of array receiving systems with internal losses," *IEEE Transactions on Antennas and Propagation*, vol. 29, no. 4, pp. 600–608, 1981.

[16] T. Wu and R. King, "The cylindrical antenna with non-reflecting resistive loading," *IEEE Transactions on Antennas and Propagation*, vol. 13, no. 3, pp. 369–373, 1965.

[17] B. D. Popović, "Theory of cylindrical antennas with arbitrary impedance loading," *Proceedings IEE*, vol. 118, no. 10, pp. 1327–1332, 1971.

[18] B. D. Popović and D. S. Paunović, "Experimental and theoretical analysis of cylindrical RC-antennas," in *Proceedings of the International Conference on Antennas and Propagation*, vol. 1, pp. 331–335, London, UK, November 1978.

[19] M. Kanda and F. X. Ries, "A broad-band isotropic real-time electric-field sensor (BIRES) using resistively loaded dipoles," *IEEE Transactions on Electromagnetic Compatibility*, vol. EMC-23, no. 3, pp. 122–132, 1981.

[20] B. D. Popović, "Synthesis of parallel cylindrical antennas with minimal coupling," *Bulletin T. LXXIII de l'Académie Serbe des Sciences et des Arts, Classe des Sciences Techniques*, vol. 16, pp. 13–24, 1980.

[21] P. L. Tokarsky, "Mutual coupling in a system of radiators with joule losses," *Radiotekhnika i Elektronika*, vol. 31, no. 9, pp. 1717–7123, 1986, in Russian.

[22] P. L. Tokarsky, "Coupling effects in resistive UWB antenna arrays," in *Proceedings of the 3rd International Conference Ultrawideband and Ultrashort Impulse Signals (UWBUSIS'06)*, pp. 188–190, Sevastopol, Ukraine, September 2006.

[23] P. L. Tokarskiy, "Coupling impedances and electric efficiencies of vertical dipoles above the ground," *Telecommunications and Radio Engineering*, vol. 53, no. 7-8, pp. 43–47, 1999.

[24] P. L. Tokarsky, "Coupling impedances and radiation efficiencies of horizontal electric dipoles placed above the earth surface," *Telecommunications and Radio Engineering*, vol. 57, no. 4, pp. 35–41, 2002.

[25] P. L. Tokarsky, "Mutual resistances between horizontal wire antennas near an interface," in *Proceedings of the 4th International Conference Antenna Theory and Technique (ICATT'03)*, pp. 161–164, Sebastopol, CA, USA, September 2003.

[26] K. F. Warnick, R. Maaskant, M. V. Ivashina, D. B. Davidson, and B. D. Jeffs, "High-sensitivity phased array receivers for radio astronomy," *Proceedings of the IEEE*, vol. 104, no. 3, pp. 607–622, 2016.

[27] K. F. Warnick and B. D. Jeffs, "Efficiencies and system temperature for a beamforming array," *IEEE Antennas and Wireless Propagation Letters*, vol. 7, pp. 565–568, 2008.

[28] J. Diao and K. F. Warnick, "Antenna loss and receiving efficiency for mutually coupled arrays," *IEEE Transactions on Antennas and Propagation*, vol. 65, no. 11, pp. 5871–5877, 2017.

[29] K. F. Warnick, R. Maaskant, M. V. Ivashina, D. B. Davidson, and B. D. Jeffs, *Phased Arrays for Radio Astronomy, Remote Sensing, and Satellite Communications*, Cambridge University Press, New York, NY, USA, 2018.

[30] C. A. Balanis, *Antenna Theory: Analysis and Design*, John Wiley & Sons, Hoboken, NJ, USA, 3rd edition, 2016.

[31] S. Silver, *Microwave Antenna Theory and Design*, McGraw-Hill, New York, NY, USA, 1949.

[32] 4NEC2–NEC Based Antenna Modeler and Optimizer by Arie Voors, http://www.qsl.net/4nec2/.

[33] G. J. Burke and A. G. Poggio, *Numerical Electromagnetic Code (NEC). Pt. II. Program Description–Code*, Lawrence Livermore National Laboratory, Livermore, CA, USA, 1981.

[34] P. L. Tokarsky and S. N. Yerin, "A multiport approach to modeling of phased antenna array for radio astronomy," in *Proceedings of the 43rd European Microwave Conference (EuMC 2013)*, pp. 1651–1654, Nuremberg, Germany, October 2013.

[35] P. L. Tokarsky and S. N. Yerin, "Mutual coupling between antennas used as array elements for a low frequency radio telescope," in *Proceedings of the 9th International Conference Antenna Theory and Technique (ICATT'2013)*, pp. 269–272, Kiev, Ukraine, September 2013.

[36] S. N. Yerin and P. L. Tokarsky, "Mutual coupling between antennas used as elements of a phased antenna array for the decametric wave radio telescope," *Telecommunications and Radio Engineering*, vol. 75, no. 4, pp. 285–295, 2016.

[37] F. Gantmacher, *The Theory of Matrices*, Vol. 1, Chelsea, New York, NY, USA, 1959.

[38] J. A. Stratton, *Electromagnetic Theory*, McGraw-Hill Book Company, Inc., New York, NY, USA, 1953.

[39] R. E. Collin, *Antennas and Radiowave Propagation*, McGraw-Hill Book Company, Inc., New York, NY, USA, 1985.